Journal of Solid Mechanics Vol. 17, No. 1 (2025) pp. 1-16
DOI: 10.60664/jsm.2025.3081787

Research Paper

Stress Generation Due to Moving Load on Gravitational Magneto-Elastic Orthotropic Half-Space with Parabolic Irregularity

N. Dewangan[1 *], S.A. Sahu[2], S. Chaudhary[3]

[1] *Department of Mathematics, Govt. Pt. Shyamacharan Shukla College, Dharsiwa, Raipur, Chhattisgarh, India*
[2] *Department of Mathematics and Computing, Indian Institute of Technology (Indian School of Mines), Dhanbad, India*
[3] *IIT(ISM,), Dhanbad, India*

Received 26 August 2023; Received in revised form 29 October 2024; Accepted 15 January 2025

ABSTRACT

This paper aims to calculate the compressive and tensile stresses in an irregular gravitational, magneto-elastic orthotropic half-space under a moving load at a constant speed. Expressions of normal and shear stresses have been obtained analytically in closed form. The prominent effects of irregularity depth, irregularity factor, gravity parameter and magneto-elastic coupling parameter on normal stress as well as on shear stress are computed numerically and analyzed by using graphs. Also surface plots have been made to analyze the effect of irregularity on normal and shear stress. It is observed that both normal and shear stresses are affected not only by the depth of irregularity but also affected by magneto-elastic parameter, gravity parameter and different types of irregularity like rectangular and parabolic irregularity in the medium. Some particular cases also have been obtained which is deduced from the present study and matched with the existing result. This current study may be useful in geo-mechanics and geo-engineering where stresses get developed in the irregular body frames (viz. bridges, roadways, airport runways, railway, underground railways, etc.) due to moving load which is the cause of fracture.

Keywords: Magneto-elastic; Moving load; Seismology; Solid earth physics; Irregularity.

[*]Corresponding author. Tel.: 8878427915.
E-mail address: nidhi.dewangan86@gmail.com (N. Dewangan)

1 INTRODUCTION

TO develop a better understanding of the behaviour of the media under certain load moving on the surface, produced stresses play a key role. It is therefore interesting to calculate the stresses due to moving load in medium with the variable thickness under gravity and magnetism. Over the last 20 years, studies on the moving load problems are of primary importance due to both the theoretical and practical significance. Although stress is often induced within the manufacturing process techniques such as fabrication, a far greater concern within many structures in the stress arising from external loads may also be considered. Moreover, moving loads have a significant effect on dynamic stresses in elastic structures and cause them to vibrate intensively. It may be seen that the stresses developed due to the normal moving load on the orthotropic structure can be employed to determine the strength, endurance, and durability of the structure. These investigations can be utilized in many branches of modern transportation engineering, such as the design of track/road beds, parking garages, ballistic systems (i.e., rail guns), aircraft runways, high-speed precision machining, magnetic disk drives, and so forth. Irregularities may occur due to some natural or artificial phenomena, in roads, bridges, etc., possess large span but small depth. So, the problem of moving load over an irregular, gravitational orthotropic half space may be significant in the geophysical fracture. These structures are often irregular which may be of rectangular, parabolic or much-complicated irregularity shape. Stresses get affected by such irregularities, and therefore, it requires attention and analysis. These interesting facts motivated us for the present study. In the past several decades, a lot of researchers have extensively studied the dynamic response of a half-space subjected to a moving load. [Sneddon, 1952] was the first to use the method of Fourier integral transform to determine the stress distribution in half-space for the case of a normal uniform load moving steadily on the surface of an isotropic material with subsonic velocity. The steady state solution of the problem of moving normal load over an elastic half-space was given by [Cole and Huth, 1958]. Stresses developed in a transversely isotropic elastic half space due to normal moving load over a rough surface have been determined by [Mukherjee, 1969]. The problem of moving load on a plane resting on an elastic half-space has been solved by [Sackman, 1961] and [Miles, 1966]. Some notable work concerned with the problem of moving load on an elastic half-space has been done by [Achenbach *et al*., 1967],[Olsson, 1991], [Kota and Singh, 1991], [Alkeseyeva, 2007], etc. [Selim, 2007] discussed the static deformation of an irregular initially stressed medium. The dynamic response of a normal moving load in the plane of symmetry of a monoclinic half-space was studied by [Chattopadhyay and Saha, 2006]. Much work has been discussed dealing with irregularity by [Chattopadhyay *et al.,* 2013]. [Singh *et al.,* 2014, 2016] studied the problem on moving load in different types of structure. [Liou and Sung, 2008] estimated the stresses in an anisotropic half-plane under a moving load applied over the surface of the half-plane at a subsonic speed. Later [Liou and Sung, 2012] investigated the response of an anisotropic half-plane under a moving load at all speeds. [Fu, 2005] has presented the integral representation of the surface-impedance tensor for incompressible elastic material using the Stroh formalism.

The extension of the earth is made up of solids, liquids and occluded gases. The solids are commonly called rocks. When mineral occurs with specific geometrical outlines, they are called crystals. Crystals are solids bounded by natural plane surfaces or faces. A variety of crystal forms are possible. The orthotropic form is one of them. Orthotropic materials are those in which the mechanical or thermal properties are unique and independent in three mutually perpendicular directions. Wood, cold-rolled steel, ceramics as well as bone exemplify orthotropic materials. Orthotropic materials have many advantages for use as aircraft structural materials, including their formability, high speed, strength and stiffness, resistance to cracking by fatigue loading and their immunity to corrosion. The effect of rotation, magnetic field, initial stress and gravity on Rayleigh waves in a homogeneous orthotropic elastic half-space have been shown by [Abd-Alla *et al.,* 2010]. The theory of generalized surface waves in a magneto-elastic half-space of orthotropic material under the influence of initial stress and gravity field was developed by [Abd-Alla *et al.,* 2004]. [Abd-Alla *et al.*, 2012] discussed the propagation of Rayleigh waves in a rotating orthotropic material elastic half-space under initial stress and gravity. The existence of Rayleigh waves in a magneto-elastic initially stressed conducting medium is given by [Datta, 1986]. [Itou, 2016] calculate the stresses produced in an orthotropic half-plane under a moving line load. Recently, some more problems on moving load have been discussed by [Bian *et al.*, 2016], [Malekzadeh and Monajjemzadeh, 2015], [Kim and Quinton, 2016], [Kiani, 2017].

The motive of this paper is to highlight the effect of gravity, irregularity depth, magneto-elastic coupling parameter and irregularity type in produced stresses due to normal moving load with constant velocity on the free surface of an irregular magneto-elastic orthotropic half-space with gravity. Expression of normal stress and shear stress are obtained in closed form. Calculated stresses and their dependence on various parameters are shown using graph the as prime outcome of the study. The response of moving load over a surface is a subject of investigation because of its possible application in determining the strength of a structure.

2 FORMULATION OF THE PROBLEM

Let us consider an irregular, magneto-elastic orthotropic half-space under gravity and shear load F moving with a constant velocity c along the free surface of the half-space. The coordinate system is taken in such a way that (z) axis is vertically downward and x axis is along the surface. We assume the irregularity with span 2a and depth l. The origin is placed at the middle point of the irregularity as shown in Fig. 1.

The equation of irregularity is

$$z = \varepsilon\chi(x), \tag{1}$$

$$\chi(x) = \begin{cases} 0, & |x| \geq a \\ \frac{2}{a}\left(a^2 - x^2\right), & |x| < a \end{cases} \tag{2}$$

where ε is the perturbation parameter, with the condition $\varepsilon = \frac{l}{2a} \ll 1$. The assumption is justified in real scenario where the span of irregularity (2a) in earth's layer is very large as compared to the depth of irregularity (l). When line load is applied to the free surface on gravitational, magneto-elastic orthotropic half-space along a line coincident with z axis, a deformation is produced in a plane strain. For a plane strain deformation, parallel to x, z plane, the components of displacement are

$u_1 = u_1(x,z,t)$, $u_2 = 0$, $u_3 = u_3(x,z,t)$ and $\frac{\partial}{\partial y} = 0$.

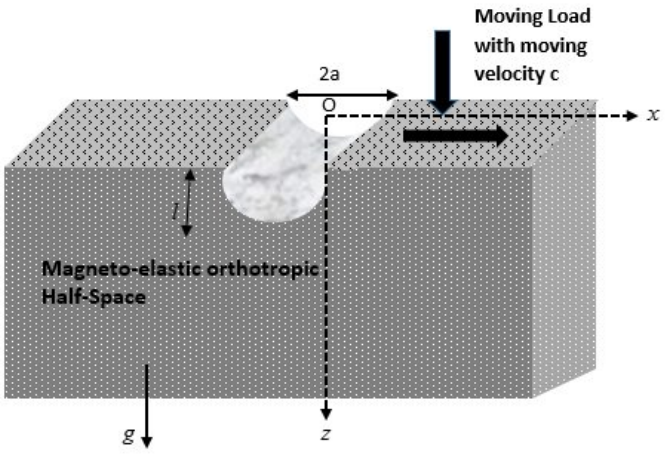

Fig. 1
Geometry of the problem.

Considering the Maxwell equations (governing by electromagnetic field) in the absence of displacement current with assumption that the medium is perfectly electric conductor [Roychoudhuri and Mukhopadhyay 2000], we have

$$\text{curl}\,\vec{h} = \vec{j} \tag{3}$$

$$\text{curl}\,\vec{E} = -\mu_e \frac{\partial \vec{h}}{\partial t} \tag{4}$$

$$\text{div}\,\vec{h} = 0 \tag{5}$$

where

$\vec{h} = curl(\vec{u} \times \overrightarrow{H_0})$ and $\overrightarrow{H} = \overrightarrow{H_0} + \vec{h}(x,z,t)$.

We have considered an orthotropic elastic solid under constant primary magnetic field $\overrightarrow{H_0}$ acting on y-direction, gravity field g and an initial compression S along the x-direction.

The dynamics of body forces may be expressed as

$X_1 = 0,\ X_3 = -g$ (where g is the acceleration due to gravity).

The compressive stress due to gravity is considered to be hydrostatic and hence, the state of initial stress T_{ij} becomes [Datta, 1986].

$$T_{11} = T_{33} = \tau \text{ and } T_{13} = 0. \tag{6}$$

The pre-stressed half-space possess the following conditions

$$\frac{\partial \tau}{\partial x} = 0 \text{ and } \frac{\partial \tau}{\partial z} - \rho g = 0. \tag{7}$$

Using equations (3), (4), (5), (6) and (7) into the three-dimensional form, we have

$$\frac{\partial T_{11}}{\partial x} + \frac{\partial T_{12}}{\partial y} + \frac{\partial T_{13}}{\partial z} - \rho g \frac{\partial \omega}{\partial x} + F_x = \rho \frac{\partial^2 u_1}{\partial t^2} \tag{8}$$

$$\frac{\partial T_{12}}{\partial x} + \frac{\partial T_{22}}{\partial y} + \frac{\partial T_{23}}{\partial z} + F_y = \rho \frac{\partial^2 u_2}{\partial t^2} \tag{9}$$

$$\frac{\partial T_{13}}{\partial x} + \frac{\partial T_{23}}{\partial y} + \frac{\partial T_{33}}{\partial z} + \rho g \frac{\partial u}{\partial x} + F_z = \rho \frac{\partial^2 u_3}{\partial t^2} \tag{10}$$

where u_1, u_2 and u_3 are the displacement components in x, y and z directions respectively, ρ is the density of the half-space , F is the Lorentz's forces.

Equations (8), (9) and (10) reduces to into two dimensions (x, z) as [Datta, 1986]

$$\frac{\partial T_{11}}{\partial x} + \frac{\partial T_{13}}{\partial z} - \rho g \frac{\partial \omega}{\partial x} + F_x = \rho \frac{\partial^2 u_1}{\partial t^2} \tag{11}$$

$$\frac{\partial T_{13}}{\partial x} + \frac{\partial T_{33}}{\partial z} + \rho g \frac{\partial u}{\partial x} + F_z = \rho \frac{\partial^2 u_3}{\partial t^2} \tag{12}$$

where

$$T_{11} = (c_{11}) \frac{\partial u_1}{\partial x} + (c_{13}) \frac{\partial u_3}{\partial z},\ T_{13} = c_{55} \left(\frac{\partial u_1}{\partial z} + \frac{\partial u_3}{\partial x} \right),\ T_{33} = c_{13} \frac{\partial u_1}{\partial x} + c_{33} \frac{\partial u_3}{\partial z}. \tag{13}$$

Using equations (1) and (2), we get

$$c_{11} \frac{\partial^2 u_1}{\partial x^2} + (c_{13} + c_{55}) \frac{\partial^2 u_3}{\partial x \partial z} + c_{55} \frac{\partial^2 u_1}{\partial z^2} - \rho g \frac{\partial u_3}{\partial x} + 2\mu_e H_0^2 \left(\frac{\partial^2 u_1}{\partial x^2} + \frac{\partial^2 u_3}{\partial x \partial z} \right) = \rho \frac{\partial^2 u_1}{\partial t^2} \tag{14}$$

$$c_{55} \frac{\partial^2 u_3}{\partial x^2} + (c_{13} + c_{55}) \frac{\partial^2 u_1}{\partial x \partial z} + c_{33} \frac{\partial^2 u_3}{\partial z^2} + \rho g \frac{\partial u_1}{\partial z} + 2\mu_e H_0^2 \left(\frac{\partial^2 u_3}{\partial z^2} + \frac{\partial^2 u_1}{\partial z \partial x} \right) = \rho \frac{\partial^2 u_3}{\partial t^2} \tag{15}$$

3 BOUNDARY CONDITIONS

The boundary condition for the motion produced by a moving load with a velocity c along x_1-axis may be written as

$$T_{13} = -F\delta(x - ct) = -F \int_0^\infty \cos k(x - ct)\, dk \qquad at \qquad z = \varepsilon\chi(x) \tag{16}$$

$$T_{33} = 0 \qquad at \qquad z = \varepsilon\chi(x) \tag{17}$$

where k and t are the wave number and time respectively and $\delta(x_1)$ is the Dirac delta function.

4 SOLUTION OF THE PROBLEM

Solution of the equations (14) and (15) may be considered as

$$u_1 = \int_0^\infty A e^{-k\xi z} \cos k\left(x - ct\right) dk, \tag{18}$$

$$u_3 = \int_0^\infty B e^{-k\xi z} \sin k\left(x - ct\right) dk, \tag{19}$$

where q is a parameter independent of k.

Introducing equations (18) and (19) into equations (14) and (15), we get

$$A\left[c_{55}\,\xi^2 + a\right] + B\left[f - qb\right] = 0, \tag{20}$$

$$A\left[f + b\xi\right] + B\left[e + \xi^2 d\right] = 0, \tag{21}$$

where

$$a = \rho c^2 - c_{11} - 2\mu_e H_0^2, b = c_{13} + c_{55} + 2\mu_e H_0^2, e = \rho c^2 - c_{55}, d = c_{33} + 2\mu_e H_0^2.$$

After solving equations (20) and (21), we have

$$\xi^4 + \zeta_1 \xi^2 + \zeta_2 = 0, \tag{22}$$

where

$$\zeta_1 = \frac{ad + c_{55}e + b^2}{c_{55}\,d} \text{ and } \zeta_2 = \frac{ae - f^2}{c_{55}\,d}.$$

Roots of equation (22) are

$$\xi_1^{\,2} = \frac{-\zeta_1 + \sqrt{\zeta_1^{\,2} - 4\zeta_2}}{2} \text{ and } \xi_2^{\,2} = \frac{-\zeta_1 - \sqrt{\zeta_1^{\,2} - 4\zeta_2}}{2}.$$

From equations (18) and (19), we get

$$u_1 = \int_0^\infty (A_1 e^{-k\xi_1 z} + A_2 e^{-k\xi_2 z}) \cos k\left(x - ct\right) dk \tag{23}$$

$$u_3 = \int_0^\infty (A_1 a_1 e^{-k\xi_1 z} + A_2 b_1 e^{-k\xi_2 z}) \sin k\left(x - ct\right) dk \tag{24}$$

where

$$a_1 = \frac{\rho c^2 - c_{11} + c_{55}\xi_1^2 - 2\mu_e H_0^2}{\left(c_{13} + c_{55}\right)\xi_1 - f + 2\mu_e H_0^2 \xi_1} \text{ and } a_2 = \frac{\rho c^2 - c_{11} + c_{55}\xi_2^2 - 2\mu_e H_0^2}{\left(c_{13} + c_{55}\right)\xi_2 - f + 2\mu_e H_0^2 \xi_2}.$$

Due to non-uniformity of the boundary, the terms A_1 and A_2 in (23) and (24) are functions of ε. We set the following approximations due to small value of ε.

$$A_1 \cong A_{10} + \varepsilon A_{11}, A_2 \cong A_{20} + \varepsilon A_{21} \tag{25}$$

Using equation (25) in equations (23) and (24), we get

$$u_1 = \int_0^\infty \left(\left(A_{10} + \varepsilon A_{11}\right) e^{-k\xi_1 z} + \left(A_{20} + \varepsilon A_{21}\right) e^{-k\xi_2 z}\right) \cos k\left(x - ct\right) dk, \tag{26}$$

$$u_3 = \int_0^\infty \left(\left(A_{10} + \varepsilon A_{11}\right) a_1 e^{-k\xi_1 z} + \left(A_{20} + \varepsilon A_{21}\right) b_1 e^{-k\xi_2 z}\right) \sin k\left(x - ct\right) dk, \tag{27}$$

Using boundary conditions and equations (13) and (14), we get

$$A_{10}\left(\xi_1 - a_1\right) + A_{20}\left(\xi_2 - b_1\right) = \frac{F}{\pi k c_{55}}, \tag{28}$$

$$A_{10}\left(\xi_1 - a_1\right) + A_{20}\left(\xi_2 - b_1\right) = A_{10}\left(\xi_1 - a_1\right) k\xi_1 \chi + A_{20}\left(\xi_2 - b_1\right) k\xi_2 \chi, \tag{29}$$

$$A_{10}P_1 + A_{20}P_2 = 0, \tag{30}$$

$$A_{10}P_1 + A_{20}P_2 = A_{10}P_1 k\xi_1\chi + A_{20}P_2 k\xi_2\chi, \tag{31}$$

after solving the equations (28) to (31), we get

$$A_{10} = \frac{FP_2}{\pi k c_{55} G}, A_{20} = \frac{-FP_1}{\pi k c_{55} G}, A_{11} = \frac{\xi_1\chi FP_2}{\pi c_{55} G}, A_{21} = \frac{\xi_2\chi FP_1}{\pi c_{55} G} \tag{32}$$

where

$$G = (\xi_1 - a_1)P_2 - (\xi_2 - b_1)P_1,$$
$$P_1 = (c_{13} + c_{33}\xi_1 a_1),$$
$$P_2 = (c_{13} + c_{33}\xi_2 b_1).$$

Substitute the value of equation (32) in equations (26) and (27), we obtained

$$u_1 = \int_0^\infty \frac{F}{\pi c_{55} G}\left(\left(\frac{P_2}{k} + \varepsilon\xi_1\chi P_2\right)e^{-k\xi_1 z} + \left(\frac{-P_1}{k} + \varepsilon\xi_2\chi P_1\right)e^{-k\xi_2 z}\right)\cos k(x - ct)\,dk, \tag{33}$$

$$u_3 = \int_0^\infty \frac{F}{\pi c_{55} G}\left(\left(\frac{P_2}{k} + \varepsilon\xi_1\chi P_2\right)a_1 e^{-k\xi_1 z} + \left(\frac{-P_1}{k} + \varepsilon\xi_2\chi P_1\right)b_1 e^{-k\xi_2 z}\right)\sin k(x - ct)\,dk, \tag{34}$$

Introducing the equations (33) and (34) into equation (13), we get the expression of the normal and shear stresses

$$\frac{T_{11}}{F} = \frac{(x_1 - ct)}{\pi c_{55} G}\left\{\frac{P_1 P_4}{Q_2}\left(1 + \frac{2x_3\varepsilon\chi\xi_2^2}{Q_2}\right) - \frac{P_2 P_3}{Q_1}\left(1 + \frac{2x_3\varepsilon\chi\xi_1^2}{Q_1}\right)\right\}, \tag{35}$$

$$\frac{T_{33}}{F} = \frac{P_1 P_2 (x_1 - ct)}{\pi c_{55} G}\left\{\left(\frac{1}{Q_2} - \frac{1}{Q_1}\right) + 2x_3\varepsilon\chi\left(\frac{\xi_2^2}{Q_2^2} - \frac{\xi_1^2}{Q_1^2}\right)\right\}, \tag{36}$$

$$\frac{T_{13}}{F} = \frac{1}{\pi G}\left\{\frac{\xi_2 P_1(\xi_2 - b_1)}{Q_2}\left(x_3 + \frac{Q_2'}{Q_2}\varepsilon\chi\right) - \frac{\xi_1 P_2(\xi_1 - a_1)}{Q_1}\left(x_3 + \frac{Q_1'}{Q_1}\varepsilon\chi\right)\right\}. \tag{37}$$

where

$$P_3 = (c_{11} + c_{13}a_1\xi_1),\ P_4 = (c_{11} + c_{13}b_1\xi_2),$$
$$Q_1 = \left\{\xi_1 x_3 + (x_1 - ct)^2\right\}, Q_2 = \left\{\xi_2 x_3 + (x_1 - ct)^2\right\},$$
$$Q_1' = \left\{\xi_1 x_3 - (x_1 - ct)^2\right\}, Q_2' = \left\{\xi_2 x_3 - (x_1 - ct)^2\right\}.$$

From equation (35) to (37), it is observed that the stress components moving with uniform velocity c in x-direction. The expression for shearing stress shows that at any plane parallel to the boundary, shearing stress attains the maximum value at $x = ct$, i.e., at the point directly below the point of application of shearing load on the boundary and it is observed that normal stresses are zero at the point directly below the point on the boundary where the moving shearing load acts.

The maximum value at $z = \beta$ is given as

$$\frac{T_{13}}{F} = \frac{1}{\pi G}\left\{\frac{P_1}{\xi_2\beta}(\xi_2 - b_1) - \frac{P_2}{\xi_1\beta}(\xi_1 - a_1)\right\} + \frac{\varepsilon\chi}{\pi G}\left\{\frac{P_1}{\xi_2\beta^2}(\xi_2 - b_1) - \frac{P_2}{\xi_1\beta^2}(\xi_1 - a_1)\right\}.$$

5 PARTICULAR CASES

***Case 1**:*

When half-space is irregular i.e. $(\varepsilon = 0)$, then equation (35) to (37), reduces to

$$\frac{T_{11}}{F}=\frac{(x-ct)}{\pi c_{55}G}\left\{\frac{P_1P_4}{Q_2}-\frac{P_2P_3}{Q_1}\right\}, \tag{38}$$

$$\frac{T_{33}}{F}=\frac{P_1P_2(x-ct)}{\pi c_{55}G}\left\{\left(\frac{1}{Q_2}-\frac{1}{Q_1}\right)\right\}, \tag{39}$$

$$\frac{T_{13}}{F}=\frac{1}{\pi G}\left\{\frac{\xi_2P_1z(\xi_2-b_1)}{Q_2}-\frac{\xi_1P_2z(\xi_1-a_1)}{Q_1}\right\}. \tag{40}$$

Equation (38) to (40) gives the expression for normal and shear stresses due to moving load on the free surface of gravitational, magneto-elastic orthotropic elastic half- space.

Case 2:

If the gravity is removed i.e. $(f=0)$, then from equation (35) to (37) we get

$$\frac{T_{11}}{F}=\frac{(x-ct)}{\pi c_{55}G''}\left\{\frac{P_1''P_4''}{Q_2}\left(1+\frac{2z\varepsilon\chi\xi_2^2}{Q_2}\right)-\frac{P_2''P_3''}{Q_1}\left(1+\frac{2z\varepsilon\chi\xi_1^2}{Q_1}\right)\right\}, \tag{41}$$

$$\frac{T_{33}}{F}=\frac{P_1''P_2''(x-ct)}{\pi c_{55}G''}\left\{\left(\frac{1}{Q_2}-\frac{1}{Q_1}\right)+2z\varepsilon\chi\left(\frac{\xi_2^{\,2}}{Q_2^{\,2}}-\frac{\xi_1^{\,2}}{Q_1^{\,2}}\right)\right\}, \tag{42}$$

$$\frac{T_{13}}{F}=\frac{1}{\pi G''}\left\{\frac{\xi_2P_1''(\xi_2-b_1'')}{Q_2}\left(z+\frac{Q_2'}{Q_2}\varepsilon\chi\right)-\frac{\xi_1P_2''(\xi_1-a_1'')}{Q_1}\left(z+\frac{Q_1'}{Q_1}\varepsilon\chi\right)\right\}. \tag{43}$$

where

$a_1''=\dfrac{\rho c^2-c_{11}+c_{55}\xi_1^2-2\mu_eH_0^2}{(c_{13}+c_{55})\xi_1+2\mu_eH_0^2\xi_1}$ and $a_2''=\dfrac{\rho c^2-c_{11}+c_{55}\xi_2^2-2\mu_eH_0^2}{(c_{13}+c_{55})\xi_2+2\mu_eH_0^2\xi_2}$.

$G=(\xi_1-a_1'')P_2''-(\xi_2-b_1'')P_1''$,

$P_1=(c_{13}+c_{33}\xi_1a_1'')$,

$P_2=(c_{13}+c_{33}\xi_2b_1'')$.

$P_3=(c_{11}+c_{13}a_1''\xi_1)$, $P_4=(c_{11}+c_{13}b_1''\xi_2)$.

Equations (41) to (43) gives the expressions of normal and shear stresses due to moving load on the free surface of irregular magneto-elastic half-space.

Case 3:

When magneto-elastic coupling parameter is removed, then eq. (35) to (37), becomes

$$\frac{T_{11}}{F}=\frac{(x-ct)}{\pi c_{55}G'}\left\{\frac{P_1'P_4'}{Q_2}\left(1+\frac{2z\varepsilon\chi\xi_2^2}{Q_2}\right)-\frac{P_2'P_3'}{Q_1}\left(1+\frac{2z\varepsilon\chi\xi_1^2}{Q_1}\right)\right\}, \tag{44}$$

$$\frac{T_{33}}{F}=\frac{P_1'P_2'\left(x_1-ct\right)}{\pi c_{55}G'}\left\{\left(\frac{1}{Q_2}-\frac{1}{Q_1}\right)+2z\varepsilon\chi\left(\frac{\xi_2{}^2}{Q_2{}^2}-\frac{\xi_1{}^2}{Q_1{}^2}\right)\right\}, \tag{45}$$

$$\frac{T_{13}}{F}=\frac{1}{\pi G'}\left\{\frac{\xi_2P_1'\left(\xi_2-b_1'\right)}{Q_2}\left(z+\frac{Q_2'}{Q_2}\varepsilon\chi\right)-\frac{\xi_1P_2'\left(\xi_1-a_1'\right)}{Q_1}\left(z+\frac{Q_1'}{Q_1}\varepsilon\chi\right)\right\}. \tag{46}$$

where

$a_1'=\frac{\rho c^2-c_{11}+c_{55}\xi_1^2}{\left(c_{13}+c_{55}\right)\xi_1-f}$ and $a_2'=\frac{\rho c^2-c_{11}+c_{55}\xi_2^2}{\left(c_{13}+c_{55}\right)\xi_2-f}$.

$G'=\left(\xi_1-a_1'\right)P_2'-\left(\xi_2-b_1'\right)P_1'$,

$P_1'=\left(c_{13}+c_{33}\xi_1a_1'\right)$,

$P_2'=\left(c_{13}+c_{33}\xi_2b_1'\right)$,

$P_3'=\left(c_{11}+c_{13}a_1'\xi_1\right)$, $P_4'=\left(c_{11}+c_{13}b_1'\xi_2\right)$.

Equation (44) to (46) gives the expression in irregular orthotropic half-space with gravity which is matched with [Singh et al., 2016].

6. NUMERICAL EXAMPLE AND DISCUSSION

For the considered structure, we use the following data [Prosser and Green, 1990]

$c_{11}=14.295\times10^9\ N/m^2, c_{13}=3.3\times10^9\ N/m^2, c_{33}=108.4\times10^9\ N/m^2$

$c_{55}=5.27\times10^9\ N/m^2, \rho=1422\,kg/m^2$.

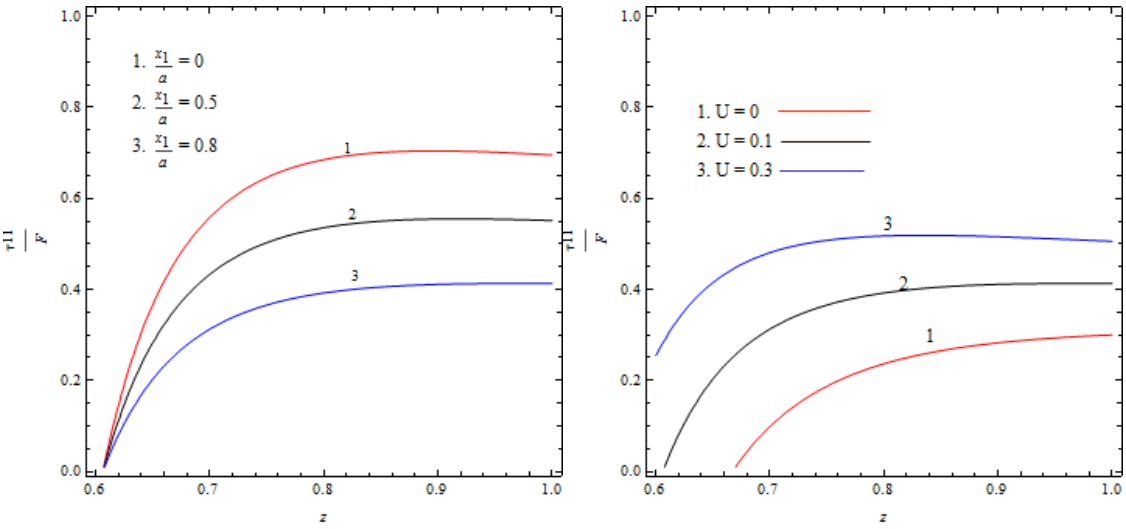

(a) (b)

Fig. 2

Variation of normal stress $\left(\frac{\tau_{11}}{F}\right)$ against depth for different irregularity depths (x_3) for different values of **(a)** irregularity factor $\left(\frac{x_1}{a}\right)$, **(b)** magneto-elastic parameter (U).

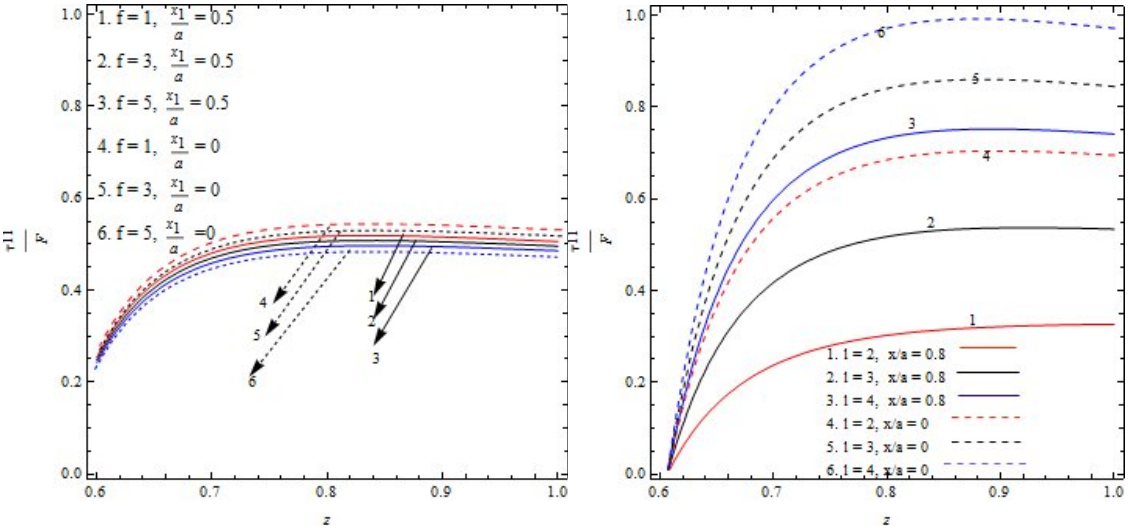

(a) (b)

Fig. 3

Variation of normal stress $\left(\frac{\tau_{11}}{F}\right)$ against depth for different irregularity depths (x_3) for different values of (a) gravitational parameter (f) and (b) irregularity depth (l) in case of parabolic irregularity as well as rectangular irregularity.

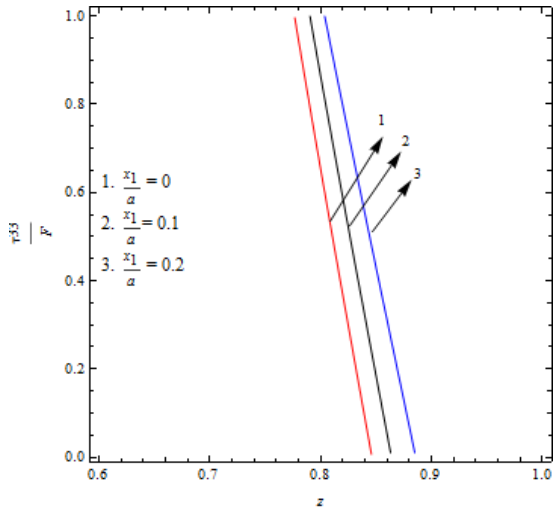

Fig. 4

Variation of normal stress $\left(\frac{\tau_{33}}{F}\right)$ against depth for different irregularity depths (x_3) for different values of irregularity factor $\left(\frac{x_1}{a}\right)$.

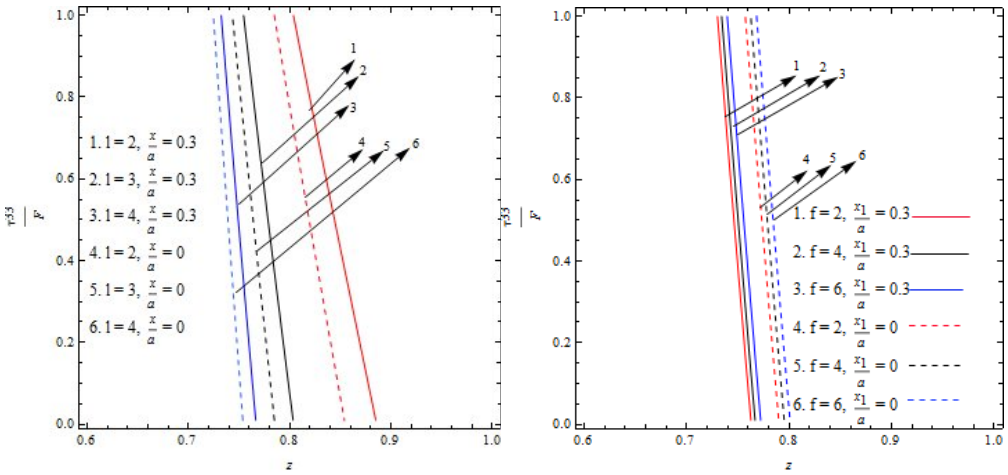

(a) (b)

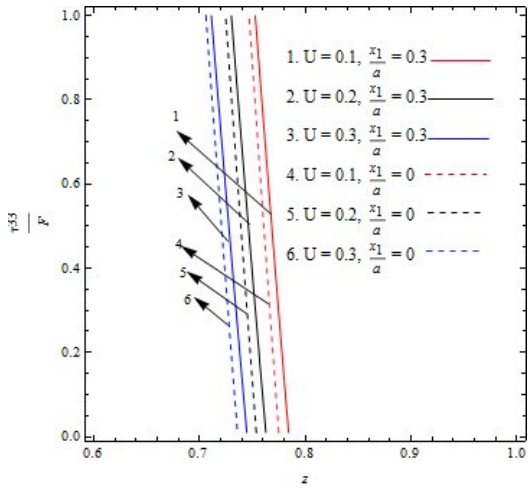

(c)

Fig. 5

Variation of normal stress $\left(\frac{\tau_{33}}{F}\right)$ against depth for different irregularity depths (z) for different values of (a) irregularity depth (l) and (b) gravitational parameter (f) (c) magneto-elastic parameter (U) in case of parabolic irregularity as well as rectangular irregularity.

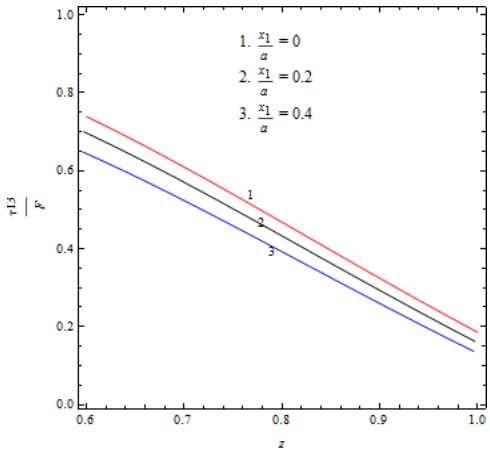

Fig. 6

Variation of normal stress $\left(\frac{\tau_{13}}{F}\right)$ against depth for different irregularity depths (z) for different values of irregularity factor $\left(\frac{x_1}{a}\right)$.

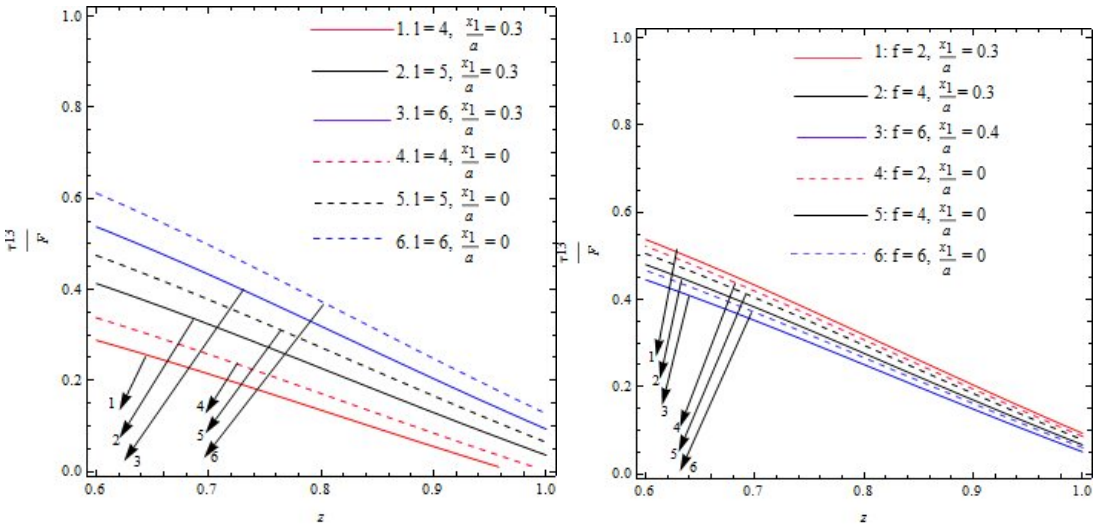

(a) (b)

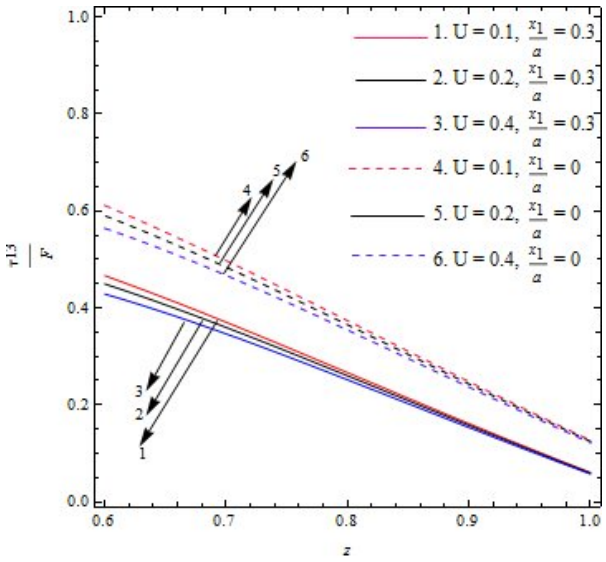

(c)

Fig. 7

Variation of normal stress $\left(\frac{\tau_{13}}{F}\right)$ against depth for different irregularity depths (z) for different values of (a) irregularity depth (l) and (b) gravitational parameter (f) (c) magneto-elastic parameter $\left(U\right)$ in case of parabolic irregularity as well as rectangular irregularity.

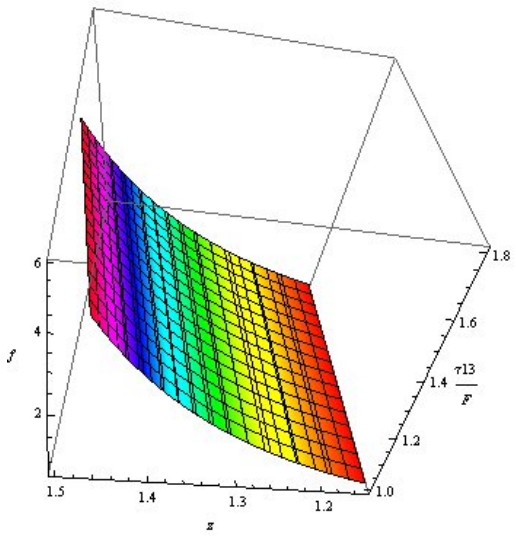

Fig. 8

Variation of shear stress $\left(\frac{\tau_{13}}{F}\right)$ against depth (z) and gravitational parameter (f) in case of parabolic irregularity.

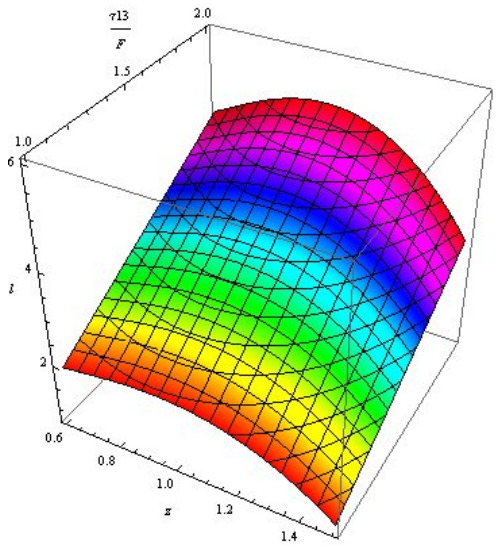

Fig. 9

Variation of shear stress $\left(\frac{\tau_{13}}{F}\right)$ against depth (z) and irregularity depth (l) in case of parabolic irregularity.

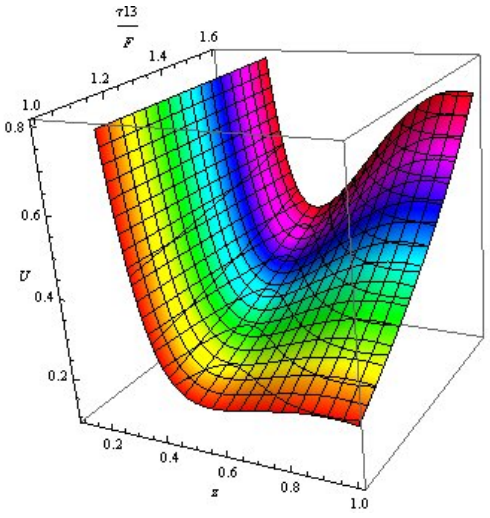

Fig. 10

Variation of shear stress $\left(\frac{\tau_{13}}{F}\right)$ against depth (z) and magneto-elastic parameter (U) in case of parabolic irregularity.

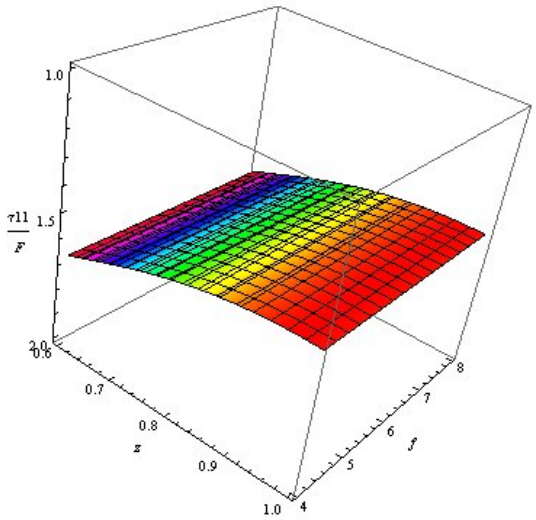

Fig. 11

Variation of normal stress $\left(\frac{\tau_{11}}{F}\right)$ against depth (z) and gravitational parameter (f) in case of parabolic irregularity.

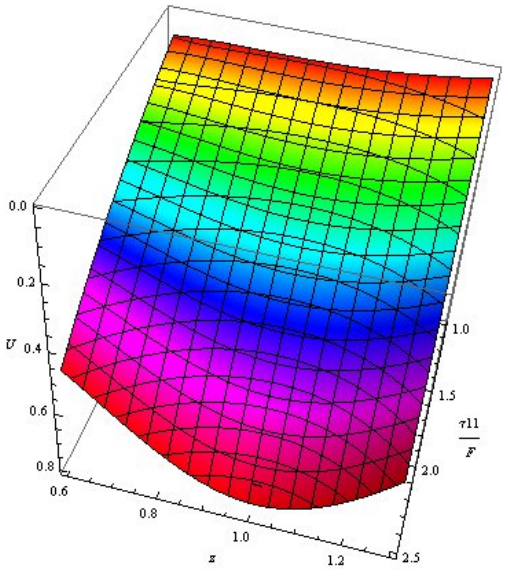

Fig. 12

Variation of shear stress $\left(\frac{\tau_{11}}{F}\right)$ against depth (z) and magneto-elastic parameter (U) in case of parabolic irregularity.

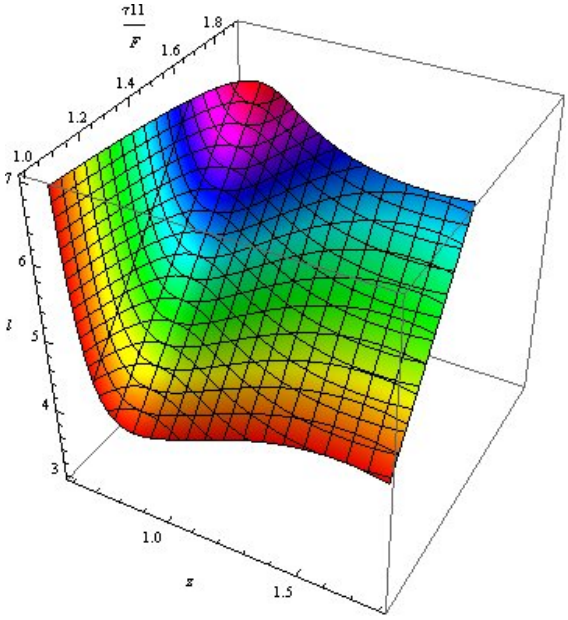

Fig. 13

Variation of shear stress $\left(\frac{\tau_{11}}{F}\right)$ against depth (z) and irregular depth (l) in case of parabolic irregularity.

7. GRAPHICAL INTERPRETATION

Figure 2(a), 2(b) and Figure 3(a), 3(b), represents the variation of normal stress $\left(\frac{\tau_{11}}{F}\right)$ with respect to the depth. It is noticed that the produced normal stress increases initially with the depth and becomes constant after a certain depth. In particular, the effect of irregularity factor $\left(\frac{x_1}{a}\right)$, magneto-elastic parameter (U), gravitational parameter (f), irregularity depth (l) and has been shown through these figures in case of parabolic irregularity as well as rectangular irregularity. It is found that the normal stress decreases with increasing value of irregularity depth, irregularity factor whereas stress increases with increasing value of gravitational parameter and magneto-elastic parameter. Fig. 3(b) elaborates a comparative study to distinctly mark the impact of type of irregularity in raised stresses. It is observed that normal stress developed due to moving load is supported more by rectangular irregularity as compared to the parabolic irregularity. In more contrast Figs. (4) and (5) help to analyse the effect of normal stress $\left(\frac{\tau_{33}}{F}\right)$ with respect to depth (z) in case of parabolic as well as rectangular irregularity. It seems that normal stress enhances with increasing values of irregularity factor and gravitational parameter and but decreases with irregularity depth and magneto-elastic parameter. Form Fig. 5(a) it is observed that normal stress developed due to moving load is supported more by parabolic irregularity as compared to the rectangular irregularity but in Fig. 5(b), rectangular irregularity is more prominent. The graphical representation for shear stress $\left(\frac{\tau_{13}}{F}\right)$ has been made through Figs. (6) and (7) in case of both parabolic and rectangle irregularities. The graphs exhibit that the increasing value irregularity factor, gravitational parameter and magneto-elastic parameter shear stress decreases. The reverse

effect of irregularity depth on the amount of produced shear stress can also be seen through same figure. In Figs. 7(a) and 7(c) it is observed that shear stress developed due to moving load is supported more by rectangular irregularity as compared to the parabolic irregularity. Surface plot of normal and shear stresses against depth, gravitational parameter, magneto-elastic parameter and irregularity depth in case of parabolic irregularity. From the surface plots (Figs. (8) to (10)), it is clear that the irregularity depth favours the developed shear stress whereas gravitational parameter and magneto-elastic parameter disfavour the developed shear stress. Surface plot (Figs. (11) to (13)) represent the variation of normal stress against depth, gravitational parameter, magneto-elastic parameter and irregular depth respectively. It is seen that the irregularity and magneto-elastic parameter support the developed normal stress whereas gravitational parameter disfavour the same.

8. CONCLUSIONS

The present study deals with the stresses developed by the moving load in an irregular, magneto-elastic orthotropic half-space under gravity. Expressions of both normal and shear stresses have been obtained in closed form. Numerical computation has been carried out for both normal and shear stresses. It is observed that both normal and shear stresses are affected significantly by the depth, irregularity factor, depth of roughness but also hit by the gravitational parameter and magneto-elastic parameter. Moreover, the present study has been made to analyze the effect of different types (shapes) of irregularity on both the stresses. Some particular cases have been obtained which is deduced from the present study and matched with existing result. Following outcomes can be pointed out as major highlights of the problem:

1. Normal stresses are zero at a point directly below the point on the boundary where moving load acts whereas shear stress attains its maximum value.
2. Normal stresses $\left(\frac{\tau_{11}}{F}\right)$ due to moving load decreases as the irregularity factor and gravitational parameter increases but it increases with increasing value of depth of irregularity and magneto-elastic parameter.
3. As compared to normal stresses $\left(\frac{\tau_{11}}{F}\right)$, normal stresses $\left(\frac{\tau_{33}}{F}\right)$ shows the reverse effect for different values of irregularity factor, gravitational parameter, depth of irregularity and magneto-elastic parameter.
4. Shear stress $\left(\frac{\tau_{13}}{F}\right)$ due to moving load decreases with increasing value of irregularity factor, gravitational parameter and magneto-elastic parameter and it disfavour for depth of irregularity.
5. Moreover, in some cases normal and shear stresses developed due to moving shear load is supported more by rectangular irregularity as compared to the parabolic irregularity. Then we conclude that both normal and shear stresses are also affected by the shape of irregularity.

The present study is likely to find application in the field of material science and engineering, aircraft engineering, etc. This current study may be useful in geo-mechanics and geo-engineering where stresses get developed in the irregular body frames (viz. bridges, roadways, airport runways, railway, underground railways, etc.) due to moving load which is the cause of fracture. Also, the magneto-elastic materials are likely to find its application in geophysical problems and certain issues in optics and acoustics. Moreover, the irregular, gravitational, magneto-elastic orthotropic media associated with a normal moving load will be a better practical insight of real earth scenario.

ACKNOWLEDGEMENT

Authors are thankful to Indian Institute of Technology (Indian School of Mines), Dhanbad for providing research facilities to Mrs. Nidhi Dewangan and Ms. Soniya Chaudhary.

REFERENCES

[1] Sneddon, I. N. [1952], "Stress Produced by a Pulse of Pressure Moving along the Surface of a Semi-Infinite Solid", Rend Circ Mat Palermo. 2, 57-62.

[2] Cole, J. and Huth J. [1958], "Stresses Produced in a Half-Plane by Moving Loads", Journal of Applied Mechanics, 25, 433-436.

[3] Mukherjee, S. [1969], "Stresses Produced by a Load Moving over a Rough Boundary of a Semi-infinite Transversely Isotropic Solid" Pure and Applied Geophysics, 72, 45-50.

[4] Sackman, J.L. [1961], "Uniformly Moving Load on a Layered Half Plane", Journal of Engineering Mechanics DivProc, 87(4), 75-89.

[5] Miles, I. W. [1966], "Response of a Layered Half-space to a Moving Load" Journal of Applied Mechanics 33, 680-681.

[6] Achenbach, J. D., Keshava, S. P. and Herrmann, G. [1967], "Moving Load on a Plate Resting on an Elastic Halfspace", Journal of Applied Mathematics and Mechanics, 34, 910-914.

[7] Olsson, M. [(1991], "On the fundamental moving load problem" Journal of Sound and Vibration, 145(2), 299-307.

[8] Kota, V.N. and Singh, V.P. [1991], "Effect of the presence of fluid on the dynamic response of buried orthotropic cylindrical shells under a moving load", Thin-Walled Structures. 12(4), 265-279.

[9] Alekseyeva, L.A. [2007], "The dynamics of an elastic half-space under the action of a moving load", Journal of Applied Mathematics and Mechanics, 71(4), 511-518.

[10] Selim, M.M. [2007], "Static deformation of an irregular initially stressed medium", Applied Mathematics and Computing, 188(2), 1274–1284.

[11] Chattopadhyay, A. and Saha, S. [2006], "Dynamic Response of Normal Moving Load in the Plane of Symmetry of A Monoclinic Half-Space", Tamkang Journal of Science and Engineering, 9(4), 307-312.

[12] Chattopadhyay, A., Gupta, S., Sahu, S.A. and Singh, A.K. [2013], "Dispersion of horizontally polarized shear waves in an irregular non-homogeneous self-reinforced crustal layer over a semi-infinite self-reinforced medium", Journal of Vibration and Control, 19(1), 109-119.

[13] Singh, A.K., Kumar, S. and Chattopadhyay, A. [2014], "Effect of irregularity and heterogeneity on the stresses produced due to a normal moving load on a rough monoclinic half-space", Meccanica, 49(12), 2861-2878 .

[14] Singh, A.K., Lakshman, A. and Chattopadhyay, A. [2016], "Effect of irregularity and anisotropy on the dynamic response due to a shear load moving on an irregular orthotropic half-space under influence of gravity", Multidiscipline Modeling in Materials and Structures, 12(1), 194-214.

[15] Liou, J.Y. and Sung, J.C. [2008], " Surface responses induced by point load or uniform traction moving steadily on an anisotropic half-plane", International Journal of Solids and Structure, 45(9) , 3219-3237.

[16] Liou, J.Y. and Sung J.C. [2012], " Supersonic responses induced by point load moving steadily on an anisotropic half-plane", International Journal of Solids and Structure, 49(17), 2254-2272.

[17] Fu, Y.B. [2005], "An integral representation of the surface-impedance tensor for incompressible elastic materials", Journal of Elasticity, 81(1), 75-90.

[18] Abd-Alla, A.M., Mahmoud, S.R., Abo-Dahab, S.M. and Helmy, M.I. [2010], "Influences of Rotation, Magnetic Field, Initial Stress, and Gravity on Rayleigh Waves in a Homogeneous Orthotropic Elastic Half-Space", Applied Mathematical Sciences, 4(2), 91 - 108.

[19] Abd-Alla, A.M.,Hammad, H.A. H. and Abo-Dahab, S.M. [2004], "Rayleigh waves in a magnetoelastic half-space of orthotropic material under influence of initial stress and gravity field", Applied Mathematics and Computing, 154(2), 583–597.

[20] Abd-Alla, A.M., Abo-Dahab, S.M. and Al-Thamali, T.A. [2012], "Propagation of Rayleigh waves in a rotating orthotropic material elastic half-space under initial stress and gravity", Journal of Mechanical Science and Technology, 26 (9), 2815-283.

[21] Datta, B. K. [1986],"Someobservationon interaction of Rayleigh waves in an elastic solid medium with the gravity field.", Rev RoumSci Tech MecAppl Tome, 31(3), 369–374.

[22] Itou, S. [2016], "Stresses produced in an orthotropic half-plane under a moving line load", International Journal of Solid and Structure, 100, 411-416.

[23] Bian, X.H., Cheng, C., Chen, Y., Chen, R. and Jiang, J. [2014], "Full-scale model testing on a ballastless high-speed railway under simulated train moving loads", Soil Dynamics and Earthquake Engineering, 66, 368-384 .

[24] Malekzadeh, P. andMonajjemzadeh, S.M. [2015], "Nonlinear response of functionally graded plates under moving load", Thin-Walled Structures, 96, 120-129.

[25] Kim, H. and Quinton, B. [2016], "Evaluation of moving ice loads on an elastic plate", Marine Structures, 50, 127-142.

[26] Kiani, Y. [2017], "Dynamics of FG-CNT reinforced composite cylindrical panel subjected to moving load"Thin-Walled Structures. 111, 48-57.

[27] S.K. Roychoudhuri, S. Mukhopadhyay [2000], "Effect of rotation and relaxation times on plane waves in generalized thermo-viscoelasticity", IJMMS 23 (7), pp.497–505

[28] Prosser, W. H. and Green, Jr. R. E. [1990], "Characterization of the nonlinear elastic properties of graphite/ epoxy composites using ultrasound" Journal of Reinforce Plastic and Computation, 9, 162-173.